

9

Electric Fields

Birgit Futterer^{1,2}, Harunori Yoshikawa³, Innocent Mutabazi³
and Christoph Egbers¹

¹Brandenburg University of Technology, Cottbus, Germany

²Otto von Guericke Universität, Magdeburg, Germany

³LOMC, UMR 6294, CNRS-Université du Havre, Le Havre, France

9.1 Convection Analog in Microgravity

Thermal convection within fluids is ubiquitous in nature and engineering. It plays a major role in heat transfer and is a main driver for geophysical and atmospheric structures. This thermally driven convection is conjoined with Archimedean buoyancy force due to the variation of the density with the temperature T in the gravitational field \vec{g} . In most of the fluids, the density decreases with the temperature and its behavior can be modeled by a linear relation for a small temperature variation: $\rho(T) = \rho_0[1 - \alpha(T - T_{ref})]$, where $\rho_0 = \rho(T_{ref})$, T_{ref} is the reference temperature, and α is the volume thermal expansion coefficient. The Archimedean buoyancy force reads

$$\vec{F} = -\rho_0 \alpha (T - T_{ref}) \vec{g} \quad (9.1)$$

Thermal convection induced by Archimedean buoyancy in the fluid layer confined between two parallel horizontal plates has been widely investigated since long time and is known as Rayleigh-Bénard convection [1]. It develops with a critical wave number $q_c = 3.117$, when the Rayleigh number $Ra = \alpha \Delta T g d^3 / \nu \kappa$ exceeds its critical value $Ra = 1707.8$ (ΔT : temperature difference between the plates, ν and κ : kinematic viscosity and thermal diffusivity of a fluid, and d : the gap between the plates).

When gravity is absent, that is in microgravity conditions, may occur no phenomena related to the Archimedean buoyancy. However, it is possible to provoke thermal convection by using an electric field coupled with a

temperature gradient applied to a fluid. This convection is often referred to as thermo-electrohydrodynamic (TEHD) convection. In fact, a dielectric fluid in the electric field \vec{E} pertains to a ponderomotive force, the density of which is given by [2]

$$\vec{F} = \rho_f \vec{E} - \frac{1}{2} \vec{E}^2 \vec{\nabla} \varepsilon + \vec{\nabla} \left[\rho \left(\frac{\partial \varepsilon}{\partial \rho} \right)_T \frac{\vec{E}^2}{2} \right] \quad (9.2)$$

where ρ_f is the free charge density. The first term is the Coulomb force density, the second term is called dielectrophoretic (DEP) force density, and the last one is the electrostriction force density. In case of incompressible fluid motion without interface, the last term can be lumped into the pressure term of the momentum equation. Thermo-electrohydrodynamics has been used as an active method for heat transfer enhancement [3, 4].

9.1.1 Conditions of DEP Force Domination

The spatial distribution of free charges varies under an electric field. This variation process occurs with a timescale $\tau_e = \varepsilon/\sigma$ called the charge relaxation time, where σ is the electric conductivity of the fluid. In dc electric field or ac electric field with a frequency $f < \tau_e^{-1}$, free charges accumulate at locations where σ varies in space, for example, at the surface of the fluid, and the Coulomb force density is often dominant component in (9.2). When the electric field is alternating at frequency $f \gg \tau_e^{-1}$, then no free charge accumulation occurs. If the frequency is also higher than the inverse of the viscous relaxation timescale $\tau_\nu = d^2/\nu$, only the time-averaged components of (9.2) are concerned with the electrohydrodynamics so that the Coulomb force has no influence on it. Then, the DEP force, which always contains a static component, drives the electrohydrodynamics. For electric field frequency $f = 50 \text{ Hz}$, the relaxation times τ_e and τ_ν should be larger than 0.02 s.

Assuming the linear variation of the dielectric permittivity with temperature, that is $\varepsilon(T) = \varepsilon_{ref}[1 - \alpha_e(T - T_{ref})]$, the dielectrophoretic force can be reduced, after removing a gradient force component, to

$$\vec{F} = -\rho_0 \alpha_e (T - T_{ref}) \vec{g}_e \quad (9.3)$$

where we have introduced the electric gravity given by [5, 6]

$$\vec{g}_e = \nabla \left[\frac{\varepsilon_{ref} \alpha_e \vec{E}^2}{2\rho_0 \alpha} \right]. \quad (9.4)$$

The electric gravity represents the gradient of the electrostatic energy stored in the dielectric fluid.

This TEHD convection driven by the DEP force in microgravity is the subject of this chapter. The chapter is organized as follows: After introducing the physical basis of the TEHD convection, we will discuss the electric gravity in three classic shapes of capacitors and then equations governing the convection development from the quiescent conductive state of the fluid. The chapter will end on some results from stability analysis and open questions and, additionally, will give a short summary on application in extended microgravity experiments.

9.1.2 Equations Governing DEP-Driven TEHD Convection

We consider a dielectric fluid confined inside a capacitor with applied alternating voltage $V(t) = \sqrt{2} V_0 \cdot \sin(2\pi ft)$. The TEHD convection in microgravity conditions may be described by mass and momentum equations coupled to energy and electric field equations. The assumption $f \gg \tau_e^{-1}, \tau_\nu^{-1}$ allows for use of the time-averaged description; that is, the electric field and, hence, the electric gravity can be averaged over a period in the governing equations. In the Boussinesq approximation, the equations for TEHD convection read

$$\vec{\nabla} \cdot \vec{u} = 0 \quad (9.5)$$

$$\frac{\partial \vec{u}}{\partial t} + (\vec{u} \cdot \vec{\nabla}) \vec{u} = -\vec{\nabla} \Pi + \nu \vec{\nabla}^2 \vec{u} - \alpha (T - T_{ref}) \vec{g}_e \quad (9.6)$$

$$\frac{\partial T}{\partial t} + (\vec{u} \cdot \vec{\nabla}) T = \kappa \vec{\nabla}^2 T \quad (9.7)$$

$$\vec{\nabla} \cdot [\varepsilon(T) \vec{\nabla} \varphi] = 0 \text{ with } \vec{E} = -\vec{\nabla} \varphi \quad (9.8)$$

where φ is the electrostatic potential.

In the energy Equation (9.7), the viscous dissipation and Joule heating have been neglected, following the arguments developed by [7]. The reduced pressure Π is given by

$$\Pi = \frac{p}{\rho_0} - \frac{\alpha_e \epsilon_{ref} (T - T_{ref}) \vec{E}^2}{2\rho_0} - \left(\frac{\partial \varepsilon}{\partial \rho} \right)_T \frac{\vec{E}^2}{2}. \quad (9.9)$$

These equations must be solved together with appropriate boundary conditions at surfaces S_i of electrodes ($i = 1, 2$):

$$\vec{u} = 0 \quad T = T_1; \quad \phi = V_0 \quad \text{at } S_1, \quad (9.10)$$

$$\vec{u} = 0 \quad T = T_2; \quad \phi = 0 \quad \text{at } S_2. \quad (9.11)$$

From now on, we will consider T_2 as the reference temperature, that is $T_{\text{ref}} = T_2$, and correspondingly, ϵ_{ref} will be referred to as $\epsilon_2 = \epsilon(T = T_2)$.

9.2 Electric Gravity in the Conductive State for Simple Capacitors

Consider a dielectric fluid at rest between electrodes in simple geometrical configurations, that is plane, cylindrical, or spherical, with a temperature difference $\Delta T = T_1 - T_2$ and an alternative tension V_0 between the electrodes S_1 and S_2 (Figure 9.1). The temperature and electric fields can be computed analytically from the Equations (9.5–9.8), whereby the electric gravity can be derived by (9.4). Table 9.1 gives the expressions for these three configurations.

In plane capacitor, the gravity is due to the thermoelectric coupling through the thermoelectric parameter $B = \alpha_e \Delta T$; it is always oriented along the temperature gradient, that is $\vec{g}_e \uparrow \uparrow \nabla T$. In cylindrical and spherical capacitors, the gravity is a product of two contributing factors: The first $g_0 (\sim r^{-n}, n = 3$ for cylindrical annulus and $n = 5$ for spherical shell) comes from the inhomogeneity of the electric field due to the curvature, and the second $F(B, \eta, r)$ is the thermoelectric coupling. Moreover, the electric gravity can be either centripetal, that is $\vec{g}_e \uparrow \downarrow \vec{e}_r$, or centrifugal

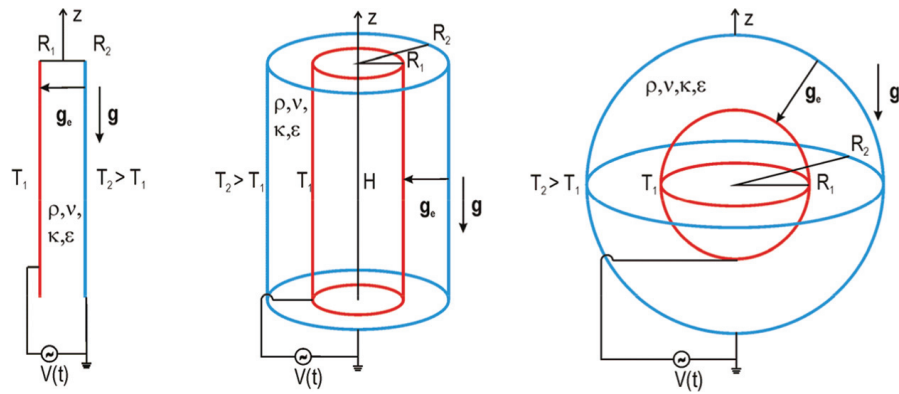


Figure 9.1 Flow configurations: plane capacitor, cylindrical annulus, and spherical shell.

Table 9.1 Basic conductive states in different electrode configurations. Parameter $B = \alpha_E \Delta T$ has been introduced

| Capacitor Shape | Temperature Field | Electric Field | Electric Gravity | |
|-----------------|---|---|---|---|
| Plane capacitor | $T(x) = T_2 + (1 - \frac{x}{d}) \Delta T$ | $\vec{E}(x) = E(x) \vec{e}_x;$ $E(x) = -E_2 [1 - B(1 - \frac{x}{d})]^{-1}$ $E_2 = \frac{B}{\ln(1-B)} \frac{V_0}{d}$ | $\vec{g}(x) = -g_0 F(B, x) \vec{e}_x; g_0 = \frac{\varepsilon_2 \alpha_E B}{\rho_0 \alpha d} (\frac{V_0}{d})^2$ $F = \left[\frac{B}{\ln(1-B)} \right]^2 \frac{1}{[1-B(1-x/d)]^3}$ | |
| | Cylindrical annulus | $T(r) = T_2 + \frac{\ln(r/R_2)}{\ln \eta} \Delta T$ | $\vec{E}(r) = E(r) \vec{e}_r;$ $E(r) = -E_2 \left[1 - B \frac{\ln(r/R_2)}{\ln \eta} \right]^{-1} \frac{R_2}{r}$ $E_2 = -\frac{B}{\ln(1-B)} \frac{V_0}{R_2 \ln \eta}$ | $\vec{g}(r) = -g_0 F(B, \eta, r) \vec{e}_r; g_0 = \frac{\varepsilon_2 \alpha_E}{\rho_0 \alpha (\ln \eta)^2} \frac{V_0^2}{r^3}$ $F = \left[\frac{B}{\ln(1+B)} \right]^2 \frac{1 - (B/(\ln \eta)) [1 + \ln(r/R_2)]}{[1 - (B/(\ln \eta)) \ln(r/R_2)]^3}$ |
| | | Spherical shell | $T(r) = T_2 + \frac{\eta}{1-\eta} \left(\frac{R_2}{r} - 1 \right) \Delta T$ | $\vec{E}(r) = E(r) \vec{e}_r;$ $E(r) = E_2 \left(\frac{R_2}{r} \right)^2 \left[1 - \frac{B\eta}{1-\eta} \left(\frac{R_2}{r} - 1 \right) \right]^{-1}$ $E_2 = -\frac{B}{\ln(1-B)} \frac{\eta}{1-\eta} \frac{V_0}{R_2}$ |

$\vec{g}_e \uparrow\uparrow \vec{e}_r$, depending upon the sign of the function $F(B, \eta, r)$. The orientation of the basic electric gravity in the spherical shell is summarized in Figure 9.2. A detailed discussion of the electric gravity in cylindrical annulus can be found in [6].

9.2.1 Linear Stability Equations and Kinetic Energy Equation

The characteristic scales can be used to introduce non-dimensional control parameters. For timescale, we chose the viscous relaxation time τ_ν , the gap d between the electrodes is chosen as length scale, and ΔT is the temperature scale. The resulting control parameters are the Prandtl number $Pr = \nu/\kappa$ and the electric Rayleigh number $L = \alpha_e \Delta T g_m d^3 / \nu \kappa$, where g_m is the electric gravity at the mid-gap and the thermoelectric parameter B .

The linearized equations near the quiescent conducting state ($\vec{u} = 0$) are as follows:

$$\vec{\nabla} \cdot \vec{u} = 0 \tag{9.12}$$

$$\frac{\partial \vec{u}}{\partial t} + (\vec{u} \cdot \vec{\nabla}) \vec{u} = -\vec{\nabla} \Pi + \vec{\nabla}^2 \vec{u} - \frac{L}{Pr} [(T - T_2) \vec{g}'_e + \theta \vec{g}_e] \tag{9.13}$$

$$Pr \left[\frac{\partial \theta}{\partial t} + (\vec{u} \cdot \vec{\nabla}) T \right] = \vec{\nabla}^2 \theta \tag{9.14}$$

$$\vec{\nabla} \left\{ [1 - B(T - T_2)] \vec{\nabla} \phi - B \theta \vec{\nabla} \varphi \right\} = 0 \tag{9.15}$$

where ϑ and ϕ denote the perturbation temperature and electric potential, respectively. Two components have been distinguished in the electric

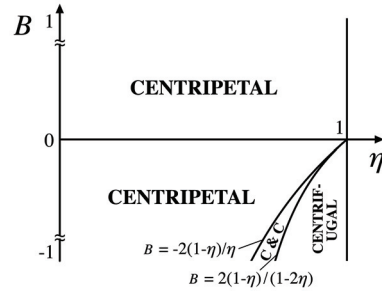


Figure 9.2 Diagram of basic gravity orientation in the spherical shell. C & C means that the gravity is centripetal and centrifugal in the inner and the outer layers, respectively.

gravity: \vec{g}_e in the basic conductive state and \vec{g}'_e related to the perturbation electric field. The latter arises through the thermoelectric coupling (9.15).

The equation of the perturbation kinetic energy is obtained straightforward from the previous equations and reads [6, 8]:

$$\frac{dK}{dt} = W_{BC} + W_{PC} - D_v \quad (9.16)$$

where

$$K = \int_V \frac{\vec{u}^2}{2} dV; \quad \text{Pr } W_{BG} = -L \int_V \theta \vec{u} \cdot \vec{g}_e dV;$$

$$\text{Pr } W_{PG} = -L \int_V [(T - T_2) \vec{u} \cdot \vec{g}'_e + \theta \vec{u} \cdot \vec{g}'_e] dV.$$

9.3 Results from Stability Analysis

9.3.1 Plane Capacitor

The TEHD convection in a dielectric fluid between two plates in microgravity has been investigated by many authors [9–13]. It has been found that the critical modes are stationary and the corresponding critical values are $L_c = 2128.696$ and $q_c = 3.226$, where q is the wave number of the perturbations in the plane of invariance. These values, which have been confirmed by different authors, are different from the critical parameters of the Rayleigh-Bénard (RB) instability: $Ra_c = 1707.8$ and $q_c = 3.117$, where $Ra = \alpha \Delta T g d^3 / \nu k$ is the Rayleigh number based on the Earth's gravity \vec{g} . Stiles has shown that application of electric potential to a stable configuration of fluid between two plates with an upward temperature gradient leads to an instability with a threshold L_c that increases with the value of $-Ra$ [12].

Recently, Yoshikawa et al. [8] revisited the problem of TEHD in a plane capacitor in microgravity by solving linear stability equations with consideration of the feedback effect of the temperature on the electric field. They showed that the difference in the critical parameters from the RB instability arises from stabilizing effects of the thermoelectric feedback through the perturbation electric gravity \vec{g}'_e ; that is, W_{PG} takes a non-negligible negative value. The sensitivity of L_c and q_c to the thermoelectric parameter B has also been found:

L_c decreases as B exceeds the value of 0.3, while the critical wave number increases.

In this work, they reported that just above the threshold of TEHD convection, the heat transfer coefficient is given by $Nu = 1 + 0.78 (L/L_c - 1)$, while for Rayleigh-Bénard convection, it is given by $Nu = 1 + 1.43(Ra/Ra_c - 1)$. This difference has been explained by the negative contribution of W_{PG} to the kinetic energy evolution: The thermoelectric feedback coupling impedes convective flow.

9.3.2 Cylindrical Capacitor

The TEHD convection in annulus has interested some researchers by the central nature of the electric buoyancy force (Table 9.1) and by its potential applications in heat transfer enhancement [3–5, 7–14]. Linear stability studies have been developed assuming the axisymmetry of convection flow. Sensitivity of the critical parameters to the direction of the temperature gradient has been found [13]. However, most of these studies assumed the small gap approximation (i.e., $\eta \sim 1$) and neglected the thermoelectric feedback.

In a recent study, Yoshikawa et al. [7] have released the small gap approximation and the assumption of axisymmetry of perturbations. They investigated the critical conditions of thermal convection for a large range of radius ratio ($0.02 < \eta < 0.999$) with the complete feedback effect. They found that the critical modes are non-axisymmetric stationary modes, although they are neither toroidal nor columnal. The critical value L_c varies significantly with η . For positive thermoelectric parameter B , the critical parameter L_c recovers the value $Ra_c = 1707.8$ of the RB instability at large η , while it converges to L_c of the plane electrode geometry (Figure 9.3). The computation of the energy generation terms W_{BG} and W_{PG} for critical modes has led to the conclusion that the basic electric gravity \vec{g}_e is the driving force of the convection: The TEHD convection is analogue to the ordinary thermal convection. The thermoelectric feedback through the perturbation gravity \vec{g}_e' has stabilizing effects and it becomes significant as $\eta \rightarrow 1$. The sensitivity of the critical parameters on curvature is analogous to that of thermal convection with centrifugal gravity in differentially heated annulus with solid rotation [15]. The TEHD convection in cylindrical annulus was observed in the experiment [5] for a small value of Ra and in a recent experiment on parabolic flight [16].

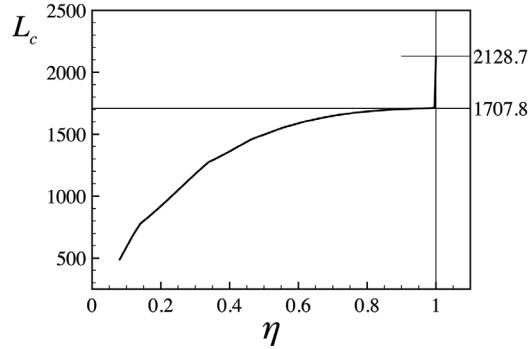


Figure 9.3 Critical electric Rayleigh number L_c for the annular geometry ($B = 10^{-4}$).

9.3.3 Spherical Shell

Rayleigh-Bénard convection in spherical shells with the condition of a radially directed gravitational buoyancy force is a general basis in geophysical flows, for example, for convective attributes in the inner Earth's mantle or core [17, 18]. Spherical laboratory experiments involving this configuration of a “self-gravitating” force field [19] will always be dominated by “natural” gravity, which is then vertically downward rather than radially inward. One alternative is to conduct the experiment in microgravity, thereby switching off the vertically upward buoyancy force. Supplementary, the application of the electric field as introduced above allows realizing a DEP-driven TEHD experiment as Rayleigh-Bénard analogue.

Travnikov et al. [20] perform a linear stability analysis for such a setup in microgravity environment varying the radius ratio h from 0.1 to 0.9. As a result, the eigenvalues are real, therewith delivering the independence of the Prandtl number (as non-dimensional parameter of the physical properties of the liquid). A lower curvature with $\eta \rightarrow 0.9$ leads to the higher critical onset of convection L_c and higher critical l -modes (e.g., $\eta = 0.3, l = 2$; $\eta = 0.5, l = 4$; $\eta = 0.7, l = 7$; $\eta = 0.9, l = 12$). Critical values for higher η are closer nearby each other. This leads to the specific design of a microgravity experiment with $\eta = 0.5$ to avoid a critical slowing down during reaching a stable convective state. Furthermore, symmetry-breaking bifurcations by means of simulations together with path-following techniques and stability computations have been applied for $\eta = 0.5$ in [21]. The patterns of convection produce different symmetries in the form of axisymmetry, octahedral, and fivefold ones. Transition to time periodic states captures a remnant tetrahedral pattern symmetry before irregular flow appears.

In both studies [20, 21], the critical L_c is referenced to the outer radius ratio. To compare it with values from the literature, we can refer to, for example, mantle models. In a very recent work, we discuss this extensively [22]. The main objective for the comparison is the r^{-5} dependency of the electric field, which is in contrast to the geophysical models. In mantles of planetary bodies, however, the gravity is taken to be constant, whereas hydrodynamic convective modes in the Earth's liquid outer core are considered with a linear dependency. But in [21–23], we conclude that the spatial dependency is not such of relevance and that the whole scenario from the onset of convection via transition to chaos is generic.

9.4 Conclusion

The thermo-electrohydrodynamic convection in dielectric fluids represents a simple way of realizing thermal convection under microgravity conditions. The present chapter has explained the main physical mechanism underlying this convection. The key role of the electric gravity was highlighted for three simple geometries of capacitors. The critical parameters depend on the geometry parameters (curvature) and on the thermoelectric parameter. For large values of thermoelectric parameter, the perturbation gravity increases the threshold of the thermal convection. The thermo-electrohydrodynamic convection in dielectric oils has been observed in experiments and might play a growing role in the heat transfer enhancement of aerospace equipment.

Acknowledgment

The authors are grateful for the bilateral PROCOPE program. The “GeoFlow” project is funded by ESA (Grant No. AO-99-049) and by the German Aerospace Center DLR (Grant No. 50WM0122 and 50WM0822). The authors would also like to thank ESA for funding the “GeoFlow” Topical Team (Grant No. 18950/05/NL/VJ). B.F. thanks the financial support by the Brandenburg Ministry of Science, Research and Culture (MWFK) as part of the International Graduate School at Brandenburg University of Technology (BTU) and the funding at the Otto von Guericke Universität Magdeburg through the Saxony-Anhalt Ministry of Culture (MK HGB/BFP). I.M. thanks the financial support from CNES (French Space Agency) and the CPER-Haute Normandie under the program THETE. H.Y. and I.M. acknowledge the financial support by

the french Agence Nationale de la Recherche (ANR), through the program “Investissements d’Avenir” (ANR-10 LABX-09-01), LABEX EMC³.

References

- [1] Chandrasekhar, S. *Hydrodynamic and Hydromagnetic Stability*. Dover Publications, 1981.
- [2] Landau L., and E. Lifshitz. *Course of Theoretical Physics—Electrodynamics of Continuous Media*, Vol. 8. Oxford: Butterworth-Heinemann, 1984.
- [3] Paschkewitz, J.S., and D.M. Pratt. “The Influence of Fluid Properties on Electrohydrodynamic Heat Transfer Enhancement in Liquids Under Viscous and Electrically Dominated Flow Conditions. *Experimental Thermal and Fluid Science* 21 (2000): 187–197.
- [4] Laohalertdecha, S., P. Naphon, and S. Wongwises. “A Review of Electrohydrodynamic Enhancement of Heat Transfer.” *Renewable Sustainable Energy Reviews* 11 (2007): 858–876.
- [5] Chandra, B., and D. Smylie. “A Laboratory Model of Thermal Convection Under a Central Force Field.” *Geophysical Fluid Dynamics* 3 (1972): 211–224.
- [6] Yoshikawa, H.N., O. Crumeyrolle, and I. Mutabazi. “Dielectrophoretic Force-Driven Thermal Convection in Annular Geometry.” *Physics of Fluids* 25 (2013): 024106.
- [7] Yavorskaya, I.M., N.I. Fomina, and Y.N. Belyaev. “A Simulation of Central Symmetry Convection in Microgravity Conditions.” *Acta Astronautica* 11 (1984): 179.
- [8] Yoshikawa, H.N., M. Tadie Fogaing, O. Crumeyrolle, and I. Mutabazi. “Dielectrophoretic Rayleigh-Bénard Convection Under Microgravity Conditions.” *Physical Review. E, Statistical, Nonlinear, and Soft Matter Physics* 87, no. 4 (2013): 043003.
- [9] Roberts, P.H. “Electrohydrodynamic Convection.” *The Quarterly Journal of Mechanics and Applied Mathematics* 22 (1969): 211–220.
- [10] Turnbull, R.J., and J. R. Melcher. “Electrohydrodynamic Rayleigh-Taylor Bulk Instability.” *Physics of Fluids* 12 (1969): 1160.
- [11] Melcher, J.R. *Continuum Electromechanics*. Massachusetts: The MIT Press, 1981.
- [12] Stiles, P.J. “Electro-Thermal Convection in Dielectric Liquids.” *Chemical Physics Letters* 179 (1991): 311–315.

- [13] Takashima, M. “Electrohydrodynamic Instability in a Dielectric Fluid Between Two Coaxial Cylinders.” *The Quarterly Journal of Mechanics and Applied Mathematics* 33 (1980): 93–103.
- [14] Stiles, P.J., and M. Kagan. “Stability of Cylindrical Couette Flow of a Radially Polarised Dielectric Liquid in a Radial Temperature Gradient.” *Physica A* 197 (1993): 583–592.
- [15] Busse, F.H., M.A. Zaks, and O. Brausch. “Centrifugally Driven Thermal Convection at High Prandtl Numbers.” *Physica D* 184 (2003): 3–20.
- [16] Dahley, N., B. Futterer, C. Egbers, O. Crumeyrolle, and I. Mutabazi. “Parabolic Flight Experiment ‘Convection in a Cylinder’ Convection Patterns in Varying Buoyancy Forces.” *Journal of Physics: Conference Series* 318 (2011): 082003.
- [17] Schubert, G., and D. Bercovici. *Treatise on Geophysics—Mantle Dynamics*. Elsevier, 2009.
- [18] Schubert, G., and P. Olson, *Treatise on Geophysics—Core Dynamics*. Elsevier, 2009.
- [19] Busse, F.H. “Convective Flows in Rapidly Rotating Spheres and Their Dynamo Action.” *Physics of Fluids* 14 (2002): 1301–1313.
- [20] Travnikov, V., C. Egbersand, R. Hollerbach. “The GEOFLOW-Experiment on ISS (Part II): Numerical Simulation.” *Advances in Space Research* 32 (2003): 181–189.
- [21] Feudel, F., K. Bergemann, L. Tuckerman, C. Egbers, B. Futterer, M. Gellert, and R. Hollerbach. “Convection Patterns in a Spherical Fluid Shell.” *Physical Review E* 83 (2011): 046304.
- [22] Futterer, B., A. Krebs, A.-C. Plesa, F. Zaussinger, D. Breuer, and C. Egbers. “Sheet-Like and Plume-Like Thermal Flow in a Spherical Convection Experiment Performed Under Microgravity.” *Journal of Fluid Mechanics* 735, (2013): DOI: 10.1017/jfm.2013.507.
- [23] Futterer, B., N. Dahley, S. Koch, N. Scurtu, and C. Egbers. “From Isoviscous Convective Experiment GeoFlow I to Temperature-Dependent Viscosity in GeoFlow II: Fluid Physics Experiments on-board ISS for the Capture of Convection Phenomena in Earth’s Outer Core and Mantle.” *Acta Astronautica* 71 (2012): 11–19.